A LOW DIMENSIONAL ANALYSIS OF A COMPLEX FLOW : A WAKE MIXING LAYER INTERACTION

Caroline Braud*, Dominique Heitz, Georges Arroyo
Cemagref,
17 Avenue de Cucill, CS 64427,
F-35044, Rennes cedex, France,
cbraud@syr.edu, dominique.heitz@cemagref.fr, georges.arroyo@cemagref.fr

J. Delville
Laboratoire d'tude Arodynamique, UMR CNRS 6609, Universit de Poitiers, ENSMA
CEAT, 43 route de l'Arodrome,
F-86036, Poitiers, France
joel.delville@lea.univ-poitiers.fr

ABSTRACT

The interaction between two canonical flows, a wake mixing layer interaction, has received recent interest (Heitz, 1999; Lamballais and Silvestrini, 2002; Braud, 2003) due to a food industry problem. The aim of this study is to extend the low dimensional analysis of this particular flow configuration. For this purpose PIV data acquired by Braud *et al.* (2004*a*) and calculations performed by Lamballais and Silvestrini (2002) are used. This work allows us to make a link between the three–dimensional organization and the secondary unsteady movement from the low velocity side to the high velocity side of the mixing Layer, appearing in this highly 3D flow configuration.

INTRODUCTION

The cross interaction between two canonical flows, the wake (see for example Williamson (1996a)) and the mixing layer (see for example Ho and Huerre, 1984), is studied here (Fig. 1). This flow configuration is of interest in many practical application like heat exchangers, off-shore structures, wind turbines, food industry (Heitz *et al.*, 2004) and others. The mean flow is made up of two mean shear directions, y and z, perpendicular to one another. This leads to a strong three dimensional organization behind the cylinder not much studied yet. A low dimensional approach is thus one of the first useful steps for an understanding of this complex phenomenon. For this flow configuration, such an approach began with Braud *et al.* (2004*a*,*c*) and will be extended here.

FLOW CONFIGURATION

A High Velocity side (HV), U_a, and Low Velocity side (LV), U_b, compose the mixing layer which impacts on the circular cylinder. The shear along the y direction from the incoming velocity leads to quasi–bidimensional structures around the z axis. The streamwise evolution of the vorticity thickness (δ_w) created by the turbulent mixing layer depends mainly on the velocity ratio $r = U_b/U_a$ (and not on the Reynolds number). When self-similarity is reached, this evolution is linear.

*Post-doctoral position at Syracuse University, NY, USA

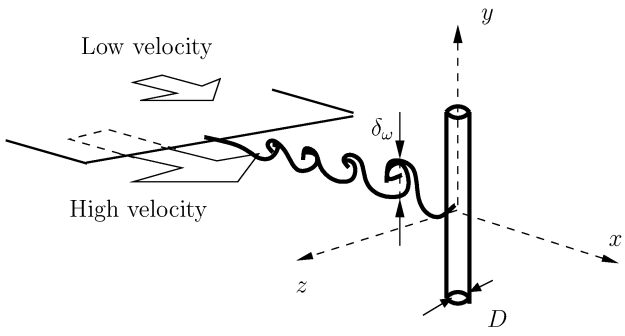

Figure 1: Flow configuration

The cylinder can thus be placed according to the parameter $\alpha = \delta_w/D$, where D is the cylinder diameter. In that way, from the definition of Woo *et al.* (1989), a shear parameter can be introduced[1], $\beta = 2\lambda/\alpha$, which includes the influence of the velocity shear of the mixing layer, $\lambda = (1-r)/(1+r)$. The aspect ratio of the cylinder is defined as L/D, where L is the length of the cylinder. An average Reynolds number $Re_m = (U_m D)/\nu$ can be defined with the average velocity of the mixing layer, $U_m = (U_a + U_b)/2$. The values of the parameters depend on the data used (see Tab. 1). For more details on the experimental set-up and the numerical calculations the reader can refer to Braud *et al.* (2004*a*) and Lamballais and Silvestrini (2002) respectively.

THREE DIMENSIONAL ORGANIZATION

The flow organization is studied in an experimental framework by means of 3 tools based on: spectra, correlations and POD mode analysis.

Spectral analysis

The first trace of this three dimensional organization of the mixing layer–wake interaction can be found when analyzing

[1] $\beta = D/U_m \times \left|\frac{\partial U}{\partial y}\right|_{max}$ and $\delta_w = \Delta U / \left|\frac{\partial U}{\partial y}\right|_{max}$ and $\Delta U = U_a - U_b$

Table 1: Parameters of the wake-mixing layer interaction from PIV measurement (Braud *et al.*, 2004*a*) and DNS calculations (Lamballais and Silvestrini, 2002)

Parameters	DNS	PIV
$L_x \times L_y \times L_z$	$28 \times 16 \times 12D^3$	$10 \times 7 \times 8D^3$
$N_x \times N_y \times N_z$	$174 \times 97 \times 144$	$45 \times 27 \times 21$
samples	420	380
dt	0.09876	–
$\lambda = \frac{1-r}{1+r}$	0.5	0.21
$r = U_b/U_a$	0.33	0.65
L/D	16	34
β	1	0,42
U_a [m/s]	1,125	18
U_b [m/s]	0,375	11.7
$Re_m = U_m D/\nu$	400	7,920

the u–velocity component measured by Hot Wire Anemometry downstream of the cylinder at (x/D=2 ; z/D=1), i.e. in the zone where the shedding of the wake of the cylinder becomes clearly evident. These results (Braud *et al.*, 2004*b*) are illustrated in Fig. 2, where this spectral distribution along the cylinder axis is plotted. In this spectral distribution one can observe two phenomena in the Interaction Area (IA), surrounded by the ellipse drawn in the figure: the first is the organization in two different frequency cells, the second is the modification of the peak width as the frequency moves from one cell to the other. The peak is broader as we go from the HV side to the center line and loses energy. This result can be interpreted as the footprint of an oblique vortex shedding. As Prasad and Williamson (1997a) found in uniform wakes, the oblique vortex shedding is associated with a broader band of the peak frequency. The spectral character thus confirms the presence of this kind of organization, associated with the inclined vortex shedding these authors identified: vortex dislocation appearing at random times. Another study from a circular cylinder in constant shear flow (Mukhopadhyay *et al.*, 2002), found slanted structures associated with dislocation and cells of constant frequency. Thus, the phenomenon studied here could be defined *a priori* as a dislocation process due to inclined vortex shedding.

The following analysis, based on two point correlations and their POD aims at providing insight into this image of the flow.

Two point Correlations

The two point correlation tensor was extracted from the measurements performed by Braud *et al.* (2004*a*) in the three dimensional domain by means of multiple PIV planes. Fig 3 shows such correlations. In these plots, the reference point corresponds to the intersection of the horizontal and vertical lines. For each plot a set of ten isocontours are shown for the positive and negative correlation values. They are equally distributed between the minimum negative and the maximum positive level. The R_{uu} correlations in the IA, plotted in the x-y–plane, (see Fig. 3-a) exhibit an asymmetric chevron pattern similar to an inclined vortex shedding on each side of the mixing layer. This pattern is also coherent with the one found if we go toward the IA from the y axis (see Fig. 3-b) where the modification of the spatial x-length scale can be attributed to the inclination.

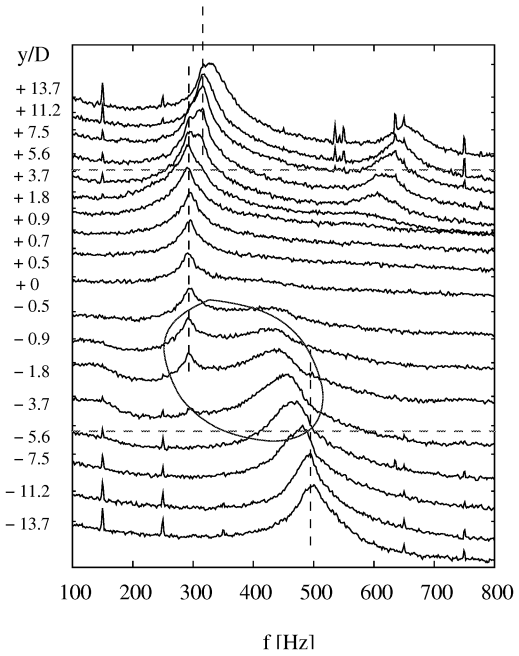

Figure 2: Spectral distribution along the cylinder at $z/D = 1$ for $Re_m = 7,920$, $L/D = 34$ and $\beta = 0.42$. PIV results, discussed in this paper, were acquired between the horizontal dotted lines. The ellipse surrounds the mean dislocation area.

The typical asymmetric chevron pattern that seems to be present, is the dominant organization that arises from the Spatial 3D POD application described in the next sections (Fig. 4-a). However, as the instantaneous behavior is strongly 3D, other steps which lead to this complex organization must exist and will be highlighted here with the higher POD modes.

POD modes

The spatial POD (Proper Orthogonal Decomposition) can be introduced briefly as a way to decompose the fluctuating velocity in a mean squares sense, as follows (for more detail the reader can refer to (Lumley, 1967; Berkooz *et al.*, 1993)):

$$u_i(\mathbf{x}, t) = \sum_n a^{(n)}(t)\Phi_i^{(n)}(\mathbf{x}) \qquad (1)$$

where $a^{(n)}$ and $\Phi_i^{(n)}$ are respectively the projection coefficient and the eigenvector of the nth POD mode. $\Phi_i^{(n)}$ comes from the resolution of an integral eigenvalue problem (Fredholm equation), where the kernel is the two point correlation tensor from a set of data (numerical or experimental). $a^{(n)}$ are then obtained from a projection of the fluctuating velocity distribution onto the POD eigenvectors. In the flow configuration studied here, all three directions are inhomogeneous which leads to a huge size of the POD kernel, $2 \times N_x \times N_y \times N_z = 56,526$ (see Braud *et al.* (2004*a*) for more details). The work presented here extends the calculation over the whole domain. For this purpose, a specific scientific library Sorensen (1996) was used.

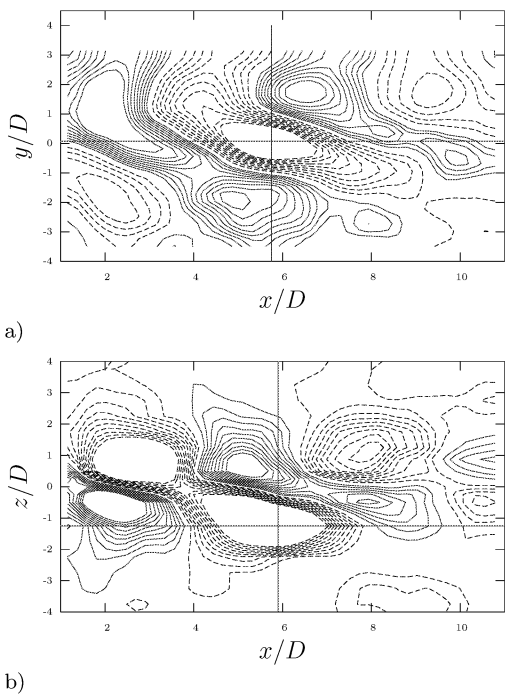

Figure 3: Positive (dotted lines) and negative (plain lines) isocontours of correlations in different planes of the 3D domain acquired by PIV measurements: a) Isocontours of R_{uu} in the IA from the z direction ($z/D = 1$); b) Isocontours of R_{uu} in the IA from the y direction ($y/D = 0$).

"Inclined structures".

PIV measurements, from which the POD was performed, were acquired between the dotted horizontal lines in Fig. 2. Figure 4-a shows the isocontour of the first component of the eigenvector for the first POD mode, $\Phi_u^{(1)}$. It shows an asymmetrical chevron pattern in good agreement with the correlation measurements (Fig. 3-a). This is in agreement with the dominance of slanted structures associated with dislocation and cells of constant frequency which was suspected from the spectral analysis, and indicates the presence of oblique shedding as was found in other three dimensional wake configuration (see for example Prasad and Williamson (1997a) in uniform wake, (Mukhopadhyay *et al.*, 2002) cylinder in a constant shear flow,...). Thus, the phenomenon studied here can be defined as a dislocation process where the first energetic step is an inclined vortex shedding, shown in a statistical footprint by the first POD mode.

Other configurations which lead to a three dimensional organization have been classified by Fiedler *et al.* (1998) in three categories: three dimensionalization which occurs from the intrinsic features of the wake (see for example Williamson (1996a)), by modification of the obstacle (see for example Lewis and Gharib, 1992), by modification of the incident flow (see for example Maull and Young, 1973). These studies will be used to understand the topologies of the higher POD modes found in the mixing layer-wake interaction.

"Longitudinal structures".

Figure 4-b shows isocontours of the seventh POD eigenvector $\Phi_u^{(7)}$. It can be observed that the shape of this mode is radically different of the previous ones. It could be associated with a statistical footprint of longitudinal structures. This is supported by the study of Maull and Young (1973) who suggest, from bluff body in a shear flow, the appearance of longitudinal structures between cells of constant frequency. Moreover, from the same flow configuration, Zhao and Ling (2003) found a longitudinal mode from a POD analysis. Further support comes from studies in uniform wakes at lower Reynolds number, where the type B instability mode, which is a longitudinal structure organization, is associated with the coexistence of two peaks of frequency. The difference here is that the coexistence of the two peaks appears in a given range of the y coordinate along the cylinder for a given average Reynolds number while in an uniform wake it appears for a given range of the Reynolds number.

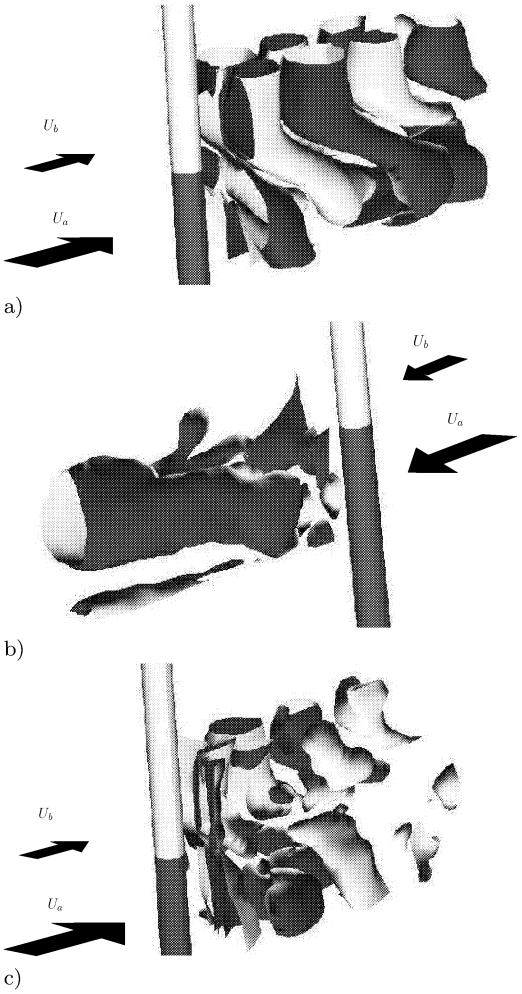

Figure 4: Isocontours of the POD 3D2C modes, positive in black and negative in white: a) first mode $\Phi_u^{(1)}$; b) seventh mode $\Phi_u^{(7)}$; c) eighth mode $\Phi_u^{(8)}$.

"Dislocation".

Figure 4-c shows isocontours of the eighth POD mode. The shape of this mode is more incoherent with a clear separation between the HV and the LV sides of the mixing layer. This mode can be associated with the appearance of disloca-

tion events. This is supported by the study of Prasad and Williamson (1997a) who found dislocation associated with a more broad frequency band similar to the one shown in the HV side of our configuration (see Fig. 2).

SECONDARY FLOW

Due to the specific pressure distribution along the obstacle, a fluid movement is initiated along the cylinder. In average, it goes from the HV side to the LV side in front of the cylinder and from the LV side to the HV side in the near wake (Heitz, 1999). It has been quantified by an average vertical velocity as high as 80% of ΔU in the near wake ($x/D \simeq 1$) and decreasing rapidly as one moves downstream, becoming equal to 30% of ΔU for $x/D \simeq 3$ (Braud, 2003).

A Spatial POD was performed from data in the $x - y$ PIV plane at $z/D = 0$, where only the velocity components in this plane where used, which we shall call POD2D-2C. Then a Galerkin projection of the Navier-Stokes equations onto the POD modes was performed to build a low order model of the dynamics of the flow in this plane (Braud *et al.*, 2004*c*). An example of an instantaneous "low order" velocity field is shown in figure 5. It is chosen at a time where $a^{(1)}(t)$ is maximum.

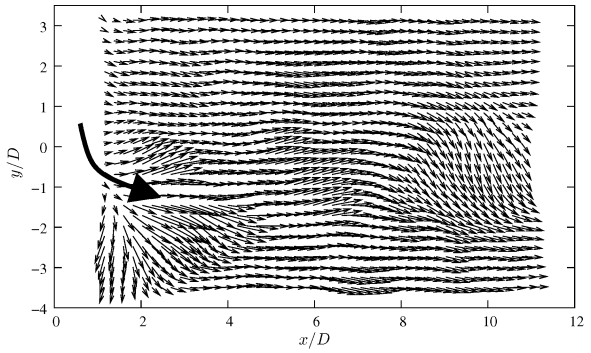

Figure 5: Instantaneous fluctuating velocity field from a 15 equation low order model of the flow ; plane z=0.

The reconstructed dynamics highlight an injection of fluid at $y/D \simeq -1$. As $\delta_w = D$ (see Tab. 1), it is equivalent to define the location of the fluid injection at $y/\delta_w \simeq -1$. The time scale of this dynamics $T = (tU_m)/D \sim 12$ is 'large' compared to the local typical time scales of the mixing layer $T \sim 7$ and high-speed and low-speed side wakes $T \sim 4$ and $T \sim 6.5$ respectively.

Until now no relation between the three dimensional organization and the secondary flow is available. This link will be highlighted here by using DNS data from Lamballais and Silvestrini (2002).

LINK BETWEEN THE 3D ORGANIZATION AND THE SECONDARY FLOW

As parameters are different in the DNS and in the experiment (Tab. 1), ($Re_m = 400$, $\beta = 1$ and $L/D = 16$), the first step is to check the validity of this comparison. The first obvious common point of these two studies is the three dimensional organization, even at the low Reynolds number for the numerical study. Other common characteristics are found in the secondary flow which has been quantified in the numerical study by the vertical mean velocity component of the same order as the experimental one, 80%ΔU at $x/D \simeq 1$. The vortex formation length is also organized in the same way, higher in the HV side than in the LV side (Heitz, 1999). Moreover, in both studies, the correlation pattern suggests an inclined vortex shedding. All these characteristics are found sufficient here to suppose a similar large scale organization.

The analysis of numerical data is focused in the x–y plane at $z/D = 0$, where the secondary flow was found dominant. A Snapshot POD analysis (Sirovich, 1989) was performed in this plane, without (POD2D-2C) and with (POD2D-3C) the third component of the velocity field taken into account.

Figure 6 shows the vector field corresponding to the first POD2D-2C mode, $\Phi_u^{(1)}$ and $\Phi_v^{(1)}$. It clearly shows the trace of a streamwise organization on each side of $y/D \simeq -2$ or more physically $y/\delta_w \simeq -1$, which can be associated with a formation of longitudinal structure. The temporal evolution associated with this first mode exhibits a low frequency and resembles the low frequency of the fluid injection found by the low order modeling (Braud *et al.*, 2004*c*).

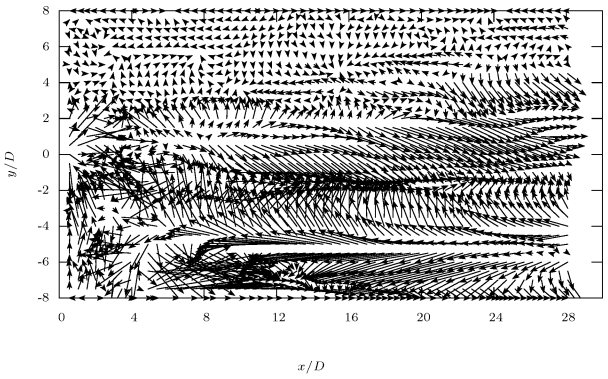

Figure 6: Fisrt mode, $\Phi_i^{(1)}$, of the POD2D-2C from DNS data in the x–y plane at z/D=0: longitudinal organization around $y/D \simeq 1$ or $y/\delta_w \simeq -1$.

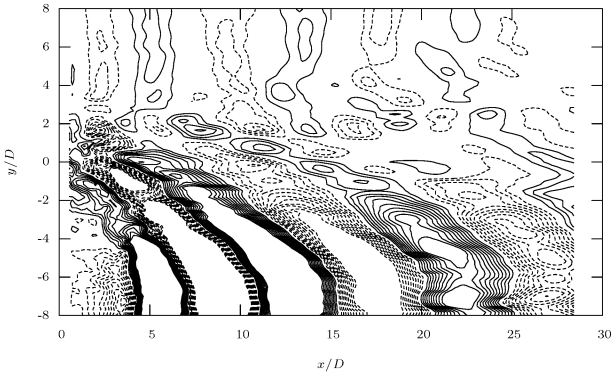

Figure 7: Isocontours of the fisrt mode of the POD2D-3C, $\Phi_w^{(1)}$, from DNS data in the x–y plane at $z/D = 0$: assymetric chevron pattern organization.

Thus this POD analysis highlights the correlation between the secondary flow behavior at low frequency and the longitudinal structure appearance. The DNS data offers the possibility of adding the third component in the POD decom-

position: POD2D-3C. Figure 7 shows the isocontours of the third component of the first POD mode, $\Phi_w^{(1)}$. The topology of this mode is associated this time with an inclined shedding organization that occurs at a higher frequency (not shown here). The secondary movement is then hidden by the inclined vortex shedding organization which is more energetic.

CONCLUSIONS

The low dimensional analysis of the interaction between two canonical flows, a wake - mixing layer interaction, has been presented here as an extension to previous approaches. A first set of conclusions was derived from a spectral analysis of Hot Wire Anemometry measurements which showed a spectral distribution evolving along the cylinder axis in a way similar to what was observed by several authors in association with inclined vortex shedding and dislocation. Plots of two point correlations gave a complement to that first step analysis, showing an asymmetric chevron pattern that was supposed to come from two inclined modes of vortex shedding on each side of the mixing layer. The use of POD decomposition allowed us, from the observation of the first most energetic modes, to confirm and further describe the dominance of slanted structures associated with dislocatons. The analysis of less energetic modes, like the seventh one, highlighted other underlying organizations among which the appearence of longitudinal structures between cells of constant frequency. By performing a Galerkin projection of the Navier-Stokes equations on the POD modes, a low order model was generated which enabled the reconstruction of a fluctuating velocity field in accordance with previous findings on the presence of an unstationary secondary flow. The results of a numerical study from Lamballais & Silvestrini were used to feed a Snapshot POD analysis with DNS data on the same kind of flow. After having verified that, despite a difference in dimensions and Reynolds number value, the main characteristics of the organization were found similar to those of the experimental work, a 2D-2C and a 2D-3C analysis were carried out to examine the link between the 3D organization and the secondary flow. A similarity was found between the temporal behavior of the longitudinal structures and that of the secondary flow. It could then be suggested that, behind the dominant pattern associated with the inclined vortex shedding lies a secondary organization made up of two low frequency fluctuating movements, a periodic fluid injection from the low to the high velocity side of the central interaction area behind the cylinder and the appearance of longitudinal structures in the same zone.

REFERENCE

Berkooz, G., Holmes, P. and Lumley, J. 1993 The proper orthogonal decomposition in the analysis of turbulent flows. *Annu. Rev. Fluid Mech.* **Vol. 25**, pp. 539–75.

Braud, C. 2003 Etude de la dynamique d'un écoulement à cisaillements croisés : interaction couche de mélange - sillage. PhD thesis, Université de Poitiers.

Braud, C., Heitz, D., Arroyo, G. and Delville, J. 2004*a* Analysis of the wake-mixing layer interaction using multiple plane piv and 3d classical pod. *Exp. in fluids* **Vol. 37**, pp. 95–104.

Braud, C., Heitz, D., Arroyo, G., Delville, J. and Bonnet, J. 2004*b* Parametric analysis of a complex flow: A mixing layer - wake interaction. In *In 57th Annual meeting of the Division of Fluid Dynamics*. Seattle - Washington, USA.

Braud, C., Heitz, D., Arroyo, G., Perret, L., Delville, J. and Bonnet, J. 2004*c* Low-dimensional analysis, using pod, for two mixing layer-wake interaction. *Int. J. of Heat and Fluid Flow* **Vol. 37**, pp. 95–104.

Fiedler, H. E., Nayeri, C., Spieweg, R. and Paschereit, C. O. 1998 Three-dimensional mixing layers and their relatives. *Exp. Thermal and Fluid Science* **Vol. 16**, pp. 3–21.

Heitz, D. 1999 Etude expérimentale du sillage d'un barreau cylindrique se développant dans une couche de mélange plane turbulente. PhD thesis, université de Poiters.

Heitz, D., Braud, C., Georgault, P., Delville, J. & Arroyo, G. 2004 Perturbation of localised ultra-clean air delivery systems. In *Food Factory of the futur - 2d International Conference*. Laval - France.

Ho, C.-M. and Huerre, P. 1984 Perturbed free shear layers. *J. Fluid Mech.* **Vol. 16**, pp. 365–424.

Lamballais, E. and Silvestrini, J. 2002 Direct numerical simulation of interactions between a mixing layer and a wake around a cylinder. *J. of Turb.* **Vol. 3**, pp. 1–21.

Lewis, C. and Gharib, M. 1992 An exploration of the wake three dimensionalities caused by a local discontinuity in cylinder diameter. *Physics of Fluids A* **Vol. 4** (1), pp. 104–117.

Lumley, J. 1967 The structure of inhomogeneous turbulent flows. In *Atmos. Turb. and Radio Wave Prop.* (ed. A. Yaglom & V. Tatarski), pp. 166–178. Nauka, Moscou.

Maull, D. and Young, R. 1973 Vortex shedding from bluff bodies in a shear flow. *J. Fluid Mech.* **Vol. 60** (2), pp. 401–409.

Mukhopadhyay, A., Venugopal, P. & Vanka, S. 2002 Oblique vortex shedding from a circular cylinder in linear shear flow. *Computers & Fluids* **31**, pp. 1–24.

Prasad, A. and Williamson, C. H. K. 1997a Three-dimensional effects in turbulent bluff-body. *J. Fluid Mech.* **Vol. 343**, pp. 235–265.

Sirovich, L. 1989 "chaotic dynamics of coherent structures". *Physica D* **Vol. 37**, pp. 126–145.

Sorensen, D. 1996 Implicitly restarted arnoldi/lanczos methods for large scale eigenvalue calculations. *Tech. Rep.*. Departement of computational and Applied Mathematics, Rice University, Houston, nASA - CR - 198342.

Williamson, C. H. K. 1996a Vortex dynamics in the cylinder wake. *Annu. Rev. Fluid Mech.* **Vol. 28**, pp. 477–539.

Woo, H., Cermak, J. and Peterka, J. 1989 Secondary flows and vortex formation around a circular cylinder in constant–shear flow. *J. Fluid Mech.* **Vol. 204**, pp. 523–542.

Zhao, H. and Ling, G. 2003 Low-dimentional dynamical systems for a wake-type shear flow with vortex dislocations. *Fluid Dynamics Research* **Vol. 33**, pp. 299–312.